Simultaneous Control of Surface Potential and Wetting of Solids with Chemisorbed Multifunctional Ligands

Merlin Bruening,[†,‡] Rami Cohen,[§] Jean François Guillemoles,[§,⊥] Tamar Moav,[†] Jacqueline Libman,[†,‖] Abraham Shanzer,*,[†] and David Cahen*,[§]

Contribution from the Departments of Organic Chemistry and Materials and Interfaces, The Weizmann Institute of Science, Rehovot 76100, Israel

Received December 27, 1996[⊗]

Abstract: Homogeneously mixed molecular assemblies of defined stoichiometry were created by adsorption of asymmetric, trifunctional ligands on gold and $CuInSe_2$ (CISe). The ligands rely on cyclic disulfide groups for binding to the substrate and can in addition possess two different substituents, one polar substituent (*p*-cyanobenzoyl or anisoyl) and one long-chain, aliphatic residue (palmitoyl). Because the substituents are covalently connected, no phase segregation will occur upon surface binding. Adsorption of these ligands on conducting surfaces changed both the surface potential (because of the polar substituent) and hydrophobicity (because of the aliphatic residue). Larger changes of surface potential were obtained by adsorption of the symmetric, dipolar ligands than by adsorption of the asymmetric ligands, and larger changes occurred on gold than on $CuInSe_2$ (up to 1.2 V between extreme modifications on Au and 0.3 V on CISe). The magnitude and direction of the observed contact potential difference changes were found to depend on the extent of coverage (as derived from electrochemical and contact angle measurements) and on the orientation of the ligands (estimated from ellipsometry and FTIR data) and could also be reconstructed using a simple, electrostatic model. These findings demonstrate that the present methodology enables simultaneous grafting of two desired properties onto solid surfaces and illustrate the predictive power of a simple, electrostatic model for molecule-controlled surface engineering.

Introduction

The surface properties of metals and semiconductors dictate many of the electronic characteristics of optoelectronic devices such as photovoltaic cells, photocathodes, detectors, and Schottky diodes.[1−3] Therefore, development of methods to control surface properties, particularly through chemical treatments, is an area of great interest.[4−18] Recently, we and others have begun to explore the potential of organic compounds for surface modification.[19−32] In ultrahigh vacuum a few ligands have been reported to induce work function changes of >1 eV.[33,34] Similarly, Evans and co-workers showed that alkanethiols and perfluorinated alkanethiols on gold yielded surface potential changes with magnitudes greater than 1.0 V.[35,36]

For the purpose of surface modifications, organic binders have *a priori* the advantages of structural versatility and flexibility.

* To whom correspondence should be addressed.

† Department of Organic Chemistry.

‡ Current address: Department of Chemistry, Texas A&M University, College Station, TX 77843-3255.

§ Department of Materials and Interfaces.

⊥ Permanent address: Laboratoire d'Electrochimie, ENSCP and CNRS, Paris, France.

‖ Deceased.

⊗ Abstract published in *Advance ACS Abstracts,* May 15, 1997.

(1) Mönch, W. *Semiconductor Surfaces and Interfaces,* 2nd ed.; Springer: Berlin, 1995; Vol. 26.

(2) Lüth, H. *Surfaces and Interaces of Solids,* 2nd ed.; Springer: Berlin, 1993.

(3) *Contacts to Semiconductors*; Brillson, L. J., Ed.; Noyes Publications: Park Ridge, NJ, 1993.

(4) Bose, D. N.; Roy, J. N.; Basu, S. *Mater. Lett.* **1984**, *2*, 455−457.

(5) Cahen, D.; Noufi, R. *Appl. Phys. Lett.* **1989**, *54*, 558−560.

(6) Cahen, D.; Noufi, R. *Solar Cells* **1991**, *30*, 53−59.

(7) Clemens, H. J.; Von Wienskowski, J.; Mönch, W. *Surf. Sci.* **1978**, *78*, 648−666.

(8) Chen, Y. F.; Tsai, C. S.; Chang, Y. H.; Chang, Y. M.; Chen, T. K.; Pang, Y. M. *Appl. Phys. Lett.* **1991**, *58*, 493−495.

(9) Chen, Y. F.; Chen, W. S. *Appl. Phys. Lett.* **1991**, *59*, 703−705.

(10) Fan, J.-F.; Oigawa, H.; Nannichi, Y. *Jpn. J. Appl. Phys.* **1988**, *27*, L1331−L1333.

(11) Fan, J.-F.; Oigawa, H.; Nannichi, Y. *Jpn. J. Appl. Phys.* **1988**, *27*, L2125−L2127.

(12) Nemirovsky, Y.; Rosenfeld, D. *J. Vac. Sci. Technol.* **1990**, *A8*, 1159−1167.

(13) Parkinson, B. A.; Heller, A.; Miller, B. *J. Electrochem. Soc.* **1979**, *126*, 954−960.

(14) Sandroff, C. J.; Nottenburg, R. N.; Bischoff, J.-C.; Bhat, R. *Appl. Phys. Lett.* **1987**, *51*, 33−35.

(15) Mandal, K. C.; Basu, S.; Bose, D. N. *J. Phys. Chem.* **1987**, *91*, 4011−4013.

(16) Yablonovitch, E.; Sandorff, C. J.; Bhat, R.; Gmitter, T. *Appl. Phys. Lett.* **1987**, *51*, 439−441.

(17) Stutzmann, M.; Herrero, C. P. *Phys. Scr.* **1989**, *T25*, 276−282.

(18) Troost, D.; Koenders, L.; Fan, L.-Y.; Mönch, W. *J. Vac. Sci. Technol.* **1987**, *B5*, 1119−1124.

(19) Bruening, M.; Moons, E.; Yaron-Marcovich, D.; Cahen, D.; Libman, J.; Shanzer, A. *J. Am. Chem. Soc.* **1994**, *116*, 2972−2977.

(20) Bruening, M.; Moons, E.; Cahen, D.; Shanzer, A. *J. Phys. Chem.* **1995**, *99*, 8368−8373.

(21) O'Regan, B.; Graetzel, M. *Nature* **1991**, *353*, 737−739.

(22) Meyer, G. J.; Leung, L. K.; Yu, J. C.; Lisensky, G. C.; Ellis, A. B. *J. Am. Chem. Soc.* **1989**, *111*, 5146−5148.

(23) Neu, D. R.; Olson, J. A.; Ellis, A. B. *J. Phys. Chem.* **1993**, *97*, 5713−5716.

(24) Murphy, C. J.; Lisensky, G. C.; Leung, L. K.; Kowach, G. R.; Ellis, A. B. *J. Am. Chem. Soc.* **1990**, *112*, 8344−8348.

(25) Lisensky, G. C.; Penn, R. L.; Murphy, C. J.; Ellis, A. B. *Science* **1990**, *248*, 840−843.

(26) Zhang, J. Z.; Ellis, A. B. *J. Phys. Chem.* **1992**, *96*, 2700−2704.

(27) Zhang, J. Z.; Geselbracht, M. J.; Ellis, A. B. *J. Am. Chem. Soc.* **1993**, *115*, 7789−7793.

(28) Lunt, S. R.; Santangelo, P. G.; Lewis, N. S. *J. Vac. Sci. Technol., B* **1991**, *9*, 2333−2336.

(29) Lunt, S. R.; Ryba, G. N.; Santangelo, P. G.; Lewis, N. S. *J. Appl. Phys.* **1991**, *70*, 7449−7467.

(30) Uchihara, T.; Matsumura, M.; Ono, J.; Tsubomura, H. *J. Phys. Chem.* **1990**, *94*, 415−418.

(31) Thackeray, J. W.; Natan, M. J.; Ng, P.; Wrighton, M. S. *J. Am. Chem. Soc.* **1986**, *108*, 3570−3577.

(32) Natan, M. J.; Thackeray, J. W.; Wrighton, M. S. *J. Phys. Chem.* **1986**, *90*, 4089−4098.

(33) Kugler, T.; Thibaut, U.; Abraham, M.; Folkers, G.; Göpel, W. *Surf. Sci.* **1992**, *260*, 64−74.

(34) Stroscio, J. A.; Bare, S. R.; Ho, W. *Surf. Sci.* **1985**, *154*, 35−51.

(35) Evans, S. D.; Ulman, A. *Chem. Phys. Lett.* **1990**, *170*, 462−466.

(36) Evans, S. D.; Urankar, E.; Ulman, A.; Ferris, N. *J. Am. Chem. Soc.* **1991**, *113*, 4121−4131.

An organic molecule can be designed to possess two elements: a surface binding group and an auxiliary functional group, each of which can be modified independently and systematically. Independent and systematic modifications of molecular functionalities, and examination of their effects on surface properties, enable (i) the development of models for surface engineering and provide (ii) a way to study semiconductor surface properties. Adopting this strategy, we recently examined benzoic and phenylhydroxamic acid derivatives as surface binding ligands.[19,20] Here the carboxylic and hydroxamic acid groups served as surface binding elements and the variable phenyl groups as polar elements that were to impart changes in the semiconductor's surface potential.[19,20] We found that these compounds indeed adsorb on semiconductor surfaces and change the semiconductor's surface potential.[19,20] The changes in surface potential were shown to be controlled by the adsorbates' properties and were found to depend linearly on their dipole moments.

In this paper we demonstrate that it is possible to modify more than a single surface property by chemisorption of tailor-made, organic molecules that possess surface binding groups and two distinctly different auxiliary groups and are capable of forming homogeneously mixed monolayers. Although many variations of this theme can be envisioned, we selected for the present work molecules that are capable of forming monolayers on semiconductors as well as on gold and whose surfaces can be readily characterized both qualitatively and quantitatively. Specifically we chose to synthesize molecules that possess a cyclic disulfide group and two different substituents, a polar residue and a hydrophobic substituent. The disulfide groups were used to guarantee surface binding to gold[37-41] and several semiconductor surfaces,[10-12,14,16,29] the polar substituents were employed to control surface potentials, and the hydrophobic residues were utilized to create a protective layer. Here we (i) characterize these molecules' assembly on gold and on $CuInSe_2$ (CISe), (ii) examine their effect on the surfaces' electron affinity and wetting properties, and (iii) reconstruct the observed changes of the surfaces' electron affinity by applying a simple, electrostatic model, which promises to become a predictive tool for surface engineering with organic molecules.

It should be emphasized that several groups previously created mixed monolayers for various purposes such as control of wetting properties, blocking of electron transfer, and use as templates.[40,42-71] These layers were usually prepared by coadsorption of different thiols on gold surfaces. This approach may, however, lead to component segregation.[45,57,58,62] Another approach to mixed monolayers involved the use of asymmetric disulfides.[38,52,56] However, if the disulfide bond cleaves to form a surface-bound thiolate, these monolayers may also segregate.[56,72] The use of asymmetric, cyclic disulfides, as introduced here, prohibits segregation of the asymmetric substituent groups even upon possible S-S bond cleavage, so as to provide stoichiometrically defined, homogeneously mixed monolayers that simultaneously control two distinct surface properties.

Experimental Section

Preparation of Ligand Assemblies. Gold films were prepared on nonpretreated p-type (100) silicon wafers (B doped 10-80 Ω·cm) which had been stored in fluoroware containers. Approximately 200-250 Å of a chromium adhesion layer was evaporated onto the wafers followed by ~1000 Å of gold (99.99%, Holland-Israel). The evaporations were performed in a cryopumped evaporator with a base pressure of ~2 × 10^{-6} mbar. The evaporator contained a liquid nitrogen-cooled trap to avoid the introduction of oil during rough pumping.

Single crystals of $CuInSe_2$ ($\rho = 10$ Ω·cm) were grown by the Bridgman-Stockbarger technique[73] and were cut along the ⟨221⟩ direction. Prior to ligand adsorption the crystals were mechanically polished with an alumina suspension (0.05 μm diameter particles) and etched for 1 min in 0.5% (v/v) Br_2/methanol. After being rinsed with methanol (analytical grade), the crystals were dipped for 1 min in an aqueous solution of 5% (w/w) KCN and 2% (w/w) KOH and rinsed with deionized water. This treatment leaves the surface free from elementary Se and In and selenium oxides.[74]

Films were formed by self-assembly. The gold films were immersed in a 1 mM solution of the ligand in acetonitrile (Merck-HPLC grade; best results are obtained when a freshly opened bottle is used) for times >18 h. After layer formation, the gold film was rinsed with acetonitrile and blown dry with nitrogen. The disulfide with two long-chain hydrocarbons (**V**) was dissolved in $CHCl_3$ because it was not soluble in acetonitrile. Accordingly, the dihydrocarbon disulfide (**V**) was first rinsed with $CHCl_3$ and then with acetonitrile. $CuInSe_2$ crystals were

(37) Nuzzo, R. G.; Allara, D. L. *J. Am. Chem. Soc.* **1983**, *105*, 4481-4483.

(38) Troughton, E. B.; Bain, C. D.; Whitesides, G. M.; Nuzzo, R. G.; Allara, D. L.; Porter, M. D. *Langmuir* **1988**, *4*, 365-385.

(39) Nuzzo, R. G.; Fusco, F. A.; Allara, D. L. *J. Am. Chem. Soc.* **1987**, *109*, 2358-2368.

(40) Bain, C. D.; Evall, J.; Whitesides, G. M. *J. Am. Chem. Soc.* **1989**, *111*, 7155-7164.

(41) Bain, C. D.; Biebuyck, H. A.; Whitesides, G. M. *Langmuir* **1989**, *5*, 723-727.

(42) Bain, C. D.; Whitesides, G. M. *Langmuir* **1989**, *5*, 1370-1378.

(43) Offord, D. A.; Griffin, J. H. *Langmuir* **1993**, *9*, 3015-3025.

(44) Zhang, L.; Lu, T.; Gokel, G. W.; Kaifer, A. E. *Langmuir* **1993**, *9*, 786-791.

(45) Folkers, J. P.; Laibinis, P. E.; Whitesides, G. M. *Langmuir* **1992**, *8*, 1330-1341.

(46) Laibinis, P. E.; Fox, M. A.; Folkers, J. P.; Whitesides, G. M. *Langmuir* **1991**, *7*, 3167-3173.

(47) Rowe, G. K.; Creager, S. E. *Langmuir* **1991**, *7*, 2307-2312.

(48) Chidsey, C. E. D.; Bertozzi, C. R.; Putvinski, T. M.; Mujsce, A. M. *J. Am. Chem. Soc.* **1990**, *112*, 4301-4306.

(49) Rubinstein, I.; Steinberg, S.; Tor, Y.; Shanzer, A.; Sagiv, J. *Nature* **1988**, *332*, 426-430.

(50) Sagiv, J. *Isr. J. Chem.* **1979**, *18*, 346-353.

(51) Lee, K. A. B.; Mowry, R.; Mclennan, G.; Finklea, H. O. *J. Electroanal. Chem. Interfacial Electrochem.* **1988**, *246*, 217-224.

(52) Offord, D. A.; John, C. M.; Griffin, J. H. *Langmuir* **1994**, *10*, 761-766.

(53) Folkers, J. P.; Laibinis, P. E.; Whitesides, G. M.; Deutch, J. *J. Phys. Chem.* **1994**, *98*, 563-571.

(54) Chailapakul, O.; Crooks, R. M. *Langmuir* **1993**, *9*, 884-888.

(55) Bertilsson, L.; Liedberg, B. *Langmuir* **1993**, *9*, 141-149.

(56) Biebuyck, H. A.; Whitesides, G. M. *Langmuir* **1993**, *9*, 1776-1770.

(57) Stranick, S. J.; Parikh, A. N.; Tao, Y.-T.; Allara, D. L.; Weiss, P. S. *J. Phys. Chem.* **1994**, *98*, 7636-7646.

(58) Laibinis, P. E.; Nuzzo, R. G.; Whitesides, G. M. *J. Phys. Chem.* **1992**, *96*, 5097-5105.

(59) Evans, S. D.; Sanassy, P. *Thin Solid Films* **1994**, *243*, 325-329.

(60) Ulman, A.; Evans, S. D.; Shnidman, Y.; Sharma, R.; Eilers, J. E.; Chang, J. C. *J. Am. Chem. Soc.* **1991**, *113*, 1499-1506.

(61) Bain, C. D.; Whitesides, G. M. *J. Am. Chem. Soc.* **1989**, *111*, 7164-7175.

(62) Takami, T.; Delamarche, E.; Michel, B.; Gerber, C.; Wolf, H.; Ringsdorf, H. *Langmuir* **1995**, *11*, 3876-3881.

(63) Rubin, S.; Chow, J. T.; Ferraris, J. P.; Zawodzinski, T. A. *Langmuir* **1996**, *12*, 363-370.

(64) Liedberg, B.; Tengvall, P. *Langmuir* **1995**, *11*, 3821-3827.

(65) Olbris, D. J.; Ulman, A.; Shnidman, Y. *J. Chem. Phys.* **1995**, *102*, 6865-6873.

(66) He, Z. L.; Bhattacharyya, S.; Cleland, W. E. J.; Hussey, C. L. *J. Electroanal. Chem.* **1995**, *397*, 305-310.

(67) Willicut, R. J.; McCarley, R. L. *Anal. Chim. Acta* **1995**, *307*, 269-276.

(68) Rowe, G. K.; Carter, M. T.; Richardson, J. N.; Murray, R. W. *Langmuir* **1995**, *11*, 1797-1806.

(69) Creager, S. E.; Clarke, J. *Langmuir* **1994**, *10*, 3675-3683.

(70) Jin, Z. H.; Vezenov, D. V.; Lee, Y. W.; Zull, J. E.; Sukenik, C. N.; Savinell, R. F. *Langmuir* **1994**, *10*, 2662-2671.

(71) Offord, D. A.; John, C. M.; Linford, M. R.; Griffin, J. H. *Langmuir* **1994**, *10*, 883-889.

(72) Fenter, P.; Eberhardt, A.; Eisenberger, P. *Science* **1994**, *266*, 1216-1218.

(73) Hornung, K. W.; Benz, K. W.; Margulis, L.; Schmid, D.; Schock, H. W. *J. Cryst. Growth* **1995**, *154*, 315-321.

(74) Moons, E. Ph.D. Thesis, The Weizmann Institute of Science, Rehovot, Israel, 1995.

immersed in a 2.5 mM solution of the ligands in acetonitrile overnight. In order to check the stability of the assembly, we rinsed the crystal with a dilute solution (0.5 mM) of the ligands and once again measured the surface potential. This rinsing did not induce significant changes (<40 mV) in the surface potential.

Characterization of Ligand Assemblies on Gold. Ellipsometry. Ellipsometric measurements were carried out following a previously described procedure.[75] Monolayer thickness was calculated using a film refractive index of $n_f = 1.45$, $k_f = 0$, with an accuracy of ±1 Å.

Electrochemical Measurements of Surface Coverage. Cu Underpotential Deposition (UPD). The electrode coverage by the symmetric and asymmetric monolayers was measured using Cu UPD.[76,77] The amount of charge passed in the UPD wave for the monolayer-covered electrode divided by the amount of charge in the UPD wave at a bare gold electrode of the same size was taken as the fraction of the gold surface not covered by the monolayer. The accuracy of the UPD coverage measurements is estimated as ±5%. The Cu UPD was carried out by cyclic voltammetry in 1 mM CuSO$_4$ + 0.1 M Na$_2$SO$_4$ solution in the range +0.400 to −0.400 V vs a mercurous sulfate reference electrode (MSE, +0.400 V vs a KCl-saturated calomel electrode), using a Solartron-Schlumberger Model 1286 potentiostat and a Houston 100 x−y recorder. The electrodes were cycled at 100 mV/s.

Contact Angle Measurements. Advancing and receding contact angles for water, deposited from a hydrophobic tip, were measured using a Ramé-Hart goniometer after measuring the work functions (1−2 h after removing the sample from the disulfide solution). The reported results are averages obtained from a total of between 5 and 10 measurements on several substrates. Of course the contact angles on hydrophilic surfaces could show some effect of contamination.

Surface Potential Measurements. Surface potential measurements were performed using a commercial Kelvin probe (Besocke Delta Phi, Jülich) in air. The method has been described elsewhere.[20,78] Surface potentials were measured immediately after layer formation. On Au the surface potential modifications, which are stable for several days, decrease after several weeks to about 2/3 of their initial value. Measurements on gold and CuInSe$_2$ represent an average from five and four different samples, respectively. The error margins for the contact potential difference (CPD) measurements are estimated to be less than about ±80 mV on Au and less than ±50 mV on CuInSe$_2$.

FTIR Measurements. FTIR (Bruker IFS66) spectra of monolayers were performed in the grazing angle mode (80° angle of incidence) with polarized light (E-vector perpendicular to the surface) using a liquid nitrogen-cooled (mercury, cadmium) telluride detector. Bare gold which had been treated with the same solvent (minus the ligands) was used as a background after a 5 min ultraviolet ozone cleaning. Immediately after the ozone cleaning, the background slide was placed in the instrument under nitrogen purging. The samples were rinsed in CHCl$_3$ immediately prior to insertion in the IR chamber. This rinsing seems to be most important for removing small hydrocarbon contaminations from the "mixed" monolayers. The cleanliness of the background is evident from the fact that ligands **I** and **III** do not show negative hydrocarbon peaks and ligand **V** does not show any spurious negative peaks in the region between 2300 and 1225 cm^{-1}. Some spectra showed broad peaks between 1200 and 1000 cm^{-1}. The reason for these peaks is unknown. No FTIR measurements of the assemblies on CuInSe$_2$ were performed due to the lack of single crystals of sufficient size.

FTIR Calculations. We used a slightly modified version of the method developed by Allara and Nuzzo[79] to calculate the orientation of ligands on the metallic surface. A full description of how to calculate the grazing angle spectrum of an isotropic layer from an isotropic transmission spectrum (including the needed computer programs) is available elsewhere.[80] We used a spectrum of the compound in KBr

to calculate the isotropic absorption coefficients of the ligands. Because the amount of compound which can be placed in a KBr pellet is very small (at high concentrations all of the radiation is absorbed at the wavelength of interest), the error in the absorption coefficient values could be as high as ±10%. The isotropic absorption coefficient for a monolayer of the material can be calculated from the concentration of ligands in the monolayer. We assumed the concentrations were 0.7 g/cm^3 for ligand **V**, 0.8 g/cm^3 for ligands **II** and **IV**, and 1.0 g/cm^3 for ligands **I** and **III**, referring to the densities of similar ligands (liquid octadecane and benzoic acid derivatives).[81] We used densities which were about 10% lower than the liquid phase densities because of the possible need to match the gold lattice. Assembly thicknesses (necessary for calculating the monolayer spectra) were estimated from the ellipsometric data of Nuzzo et al.[39] and confirmed by our own ellipsometric measurements (see Table 1). Overall errors in the estimation of absorption coefficients could be as high as 25−30% (errors of 15% in density estimation and 10% in the experimental determination of KBr spectra). For tilt angles of 55°, these errors could result in errors of 5° in the calculated angles. The refractive index of the films was calculated using the Kramers−Kronig transform. The absorbance spectrum was calculated using the method of Greenler. This method is only as good as the similarity between the molecular absorption coefficients in a monolayer and in a KBr pellet. Deviations from this assumption could occur because the ligands' environments are different in the KBr pellet and in the monolayer. If this assumption does not hold, larger errors could result.

Syntheses. Ligands III and IV (see Figure 1). A 0.5 g (0.33 mmol) sample of *trans*-1,2-dithiane-4,5-diol (racemic mixture) was dissolved in a minimum of pyridine and treated under cooling in an ice bath with 0.615 g (0.36 mmol) of 4-methoxybenzoyl chloride and 1.09 mL (0.36 mmol) of palmitoyl chloride. The mixture was allowed to stir overnight at room temperature. Then ethyl acetate was added, the organic phase was washed with 1 N aqueous HCl, 1 N aqueous NaHCO$_3$, and ice−water, dried with MgSO$_4$, and concentrated in vacuo. The crude reaction mixture was examined by TLC on silica gel and separated by column chromatography on silica gel using mixtures of hexane−methylene chloride−methanol as eluent. A yield of 690 mg (40%) of mixed disulfide (ligand **IV**) was obtained: mp 49-51 °C; ^{1}H NMR (CDCl$_3$) δ 7.94 (d, 2H, ArH), 6.90 (d, 2H, ArH), 5.21 (m, 2H, CHO), 3.85 (s, 3H, OCH$_3$), 3.2 (m, 4H, CH$_2$-S), 2.17 (m, 2H, COCH$_2$), 1.4 (m, 2H, CH$_2$-Me), 1.25 (s, 26H, aliphatic chain), 0.88 (t, 3H, −CH$_3$); IR (KBr) ν (cm^{-1}) 1743, 1714, 1606, 1270; CI MS *m/z* 373 (M − OCOC$_6$H$_4$OMe). A total of 37 mg (4.5%) of bis(4-methoxybenzoate) (ligand **III**) was also obtained: mp 119-120 °C; ^{1}H NMR (CDCl$_3$) δ 7.89 (d, 4H, ArH), 6.83 (d, 4H, ArH), 5.41 (m, 2H, CHO), 3.81 (s, 6H, OCH$_3$), 3.3 (m, 4H, CH$_2$S). IR (KBr) ν (cm^{-1}) 1716, 1606, 1513, 1264; CI MS *m/z* 421 (M + H$^+$).

Ligands I, II, and V (See Figure 1). A 1.5 g (1.0 mmol) sample of *trans*-1,2-dithiane-4,5-diol (racemic mixture) was dissolved in a minimum of pyridine and treated under cooling in an ice bath with 1.77 g (1.1 mmol) of *p*-cyanobenzoyl chloride and 3.27 mL (1.1 mmol) of palmitoyl chloride. Then dry chloroform (dried by filtration through basic alumina) was added to solubilize precipitates that had formed, and the mixture was allowed to stir overnight at room temperature. The crude mixture was diluted with chloroform, washed with 1 N aqueous HCl, water, 1 N aqueous NaHCO$_3$, and water, dried with MgSO$_4$, and concentrated. Column chromatography on silica gel using mixtures of hexane and methylene chloride as eluent provided three products. A total of 1.57 g (25%) of bis(palmitoyl ester) (ligand **V**) was obtained: mp 48-50 °C; ^{1}H NMR (CDCl$_3$) δ 5.1 (m, 2H, CHO), 3.2 (m, 4H, CH$_2$S), 2.32 (m, 4H, COCH$_2$), 1.57 (vt, 2H, CH$_2$-Me), 1.26 (s, 26H, aliphatic chain), 0.88 (t, 3H, −CH$_3$); IR (CDCl$_3$) ν (cm^{-1}) 1734 (COO); (KBr) ν (cm^{-1}) 1737, 1173; CI MS *m/z* 373 (M − OCO(CH$_2$)$_{13}$ − CH$_3$). A yield of 1.48 g (27.5%) of mixed disulfide (ligand **II**) was obtained: mp 48-50 °C; ^{1}H NMR (CDCl$_3$) δ 8.11 (d, 2H, ArH), 7.76 (d, 2H, ArH), 5.26 (m, 2H, CHO), 3.2 (m, 4H, CH$_2$S), 2.19 (m, 2H, COCH$_2$), 1.4 (m, 2H, CH$_2$-Me), 1.25 (s, 26H, aliphatic chain), 0.88 (t, 3H, −CH$_3$); IR (CDCl$_3$) ν (cm^{-1}) 2259 (CN), 1732

(75) Ron, H.; Rubinstein, I. *Langmuir* **1994**, *10*, 4566−4573.

(76) *Methods of Surface Analysis*; Christie, A. B., Ed.; Xambridge University Press: Cambridge, 1990.

(77) Kolb, D. M. In *Advances in Electrochemistry and Electrochemical Engineering*, Vol. 11; Gerischer, H., Tobias, C. W., Eds.; Wiley: New York, 1978.

(78) Surplice, N. A.; D'Archy, R. J. *J. Phys. E: Sci. Instrum.* **1970**, *3*, 477−482.

(79) Allara, D. L.; Nuzzo, R. G. *Langmuir* **1985**, *1*, 52−66.

(80) Bruening, M. *Ph.D.* Dissertation, The Weizmann Institute of Science, Rehovot, Israel, 1996.

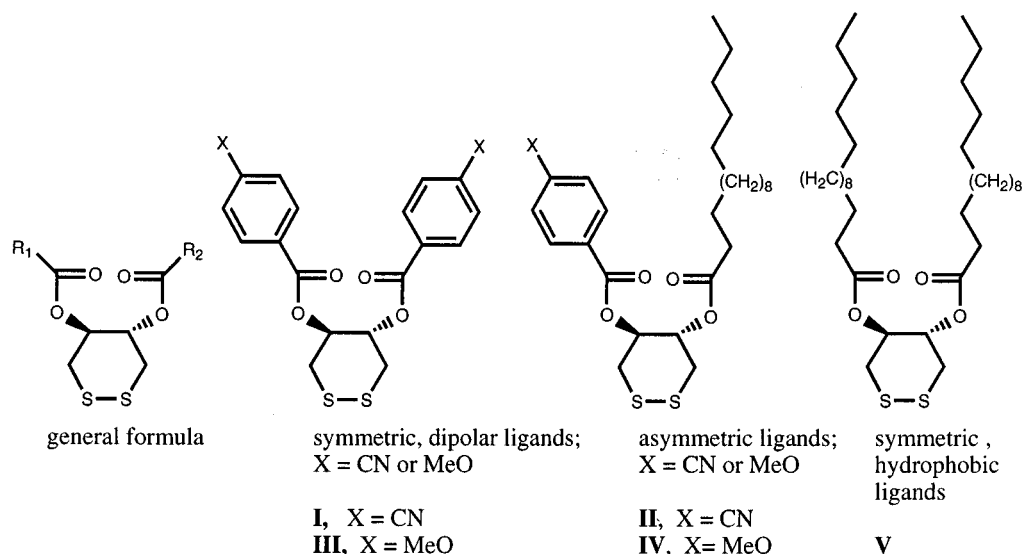(81) Weast, R. C. *CRC Handbook of Chemistry and Physics,* 52nd ed.; CRC Press: Cleveland, OH, 1972.

Figure 1. Structures of symmetric and asymmetric disulfide ligands.

Table 1. Ellipsometric Thickness, Coverage, and Contact Angles (H_2O) for Surfaces Treated with Disulfide Ligands

	disulfide ligands		ellipsom thickness (Å) on gold	surface coverage on gold[a] (%)	CAs on gold (deg)		CAs on $CuInSe_2$ (deg)	
	R1	R2			CA (adv)	CA (rec)	CA (adv)	CA (rec)
I	*p*-cyanobenzoyl	*p*-cyanobenzoyl	11 ± 1	75 ± 5	57 ± 4	40 ± 4	74 ± 1	55 ± 4
II	*p*-cyanobenzoyl	palmitoyl	15 ± 1	100 ± 5	100 ± 2	97 ± 2	95 ± 2	78 ± 4
III	anisoyl	anisoyl	9.5 ± 1	85 ± 5	70 ± 3	64 ± 3	65 ± 3	46 ± 3
IV	anisoyl	palmitoyl	14.5 ± 1	95 ± 5	98 ± 2	89 ± 3	85 ± 3	67 ± 3
V	palmitoyl	palmitoyl	21 ± 1		106 ± 2	105 ± 2	97 ± 3	83 ± 3
bare surface					70 ± 19	44 ± 30	50 ± 2	32 ± 3

[a] Coverage was determined using the underpotential deposition of copper as described in the Experimental Section on electrochemical measurements of surface coverage.

(COO); (KBr) ν (cm^{-1}) 1731, 1266; CI MS *m/z* 520 (M = H^+). A total of 520 mg (11.7%) of bis(4-cyanobenzoate) (ligand **I**) was also obtained: mp 198-200 °C; ^1H NMR ($CDCl_3$) δ 8.04 (d, 4H, ArH), 7.69 (d, 4H, ArH), 5.48 (m, 2H, CHO), 3.35 (m, 4H, CH_2S); IR ($CDCl_3$) ν (cm^{-1}) 2254 (CN), 1730 (COO); (KBr) ν (cm^{-1}) 2230, 1734, 1721, 1280; CI MS *m/z* 411 (M + H^+).

Results and Discussion

For the simultaneous modification of surface potentials and hydrophobicity of a conductor (gold) and of a semiconductor ($CuInSe_2$), we selected cyclic disulfides as surface binders and substituted them with benzoyl derivatives and palmitoyl moieties (Figure 1). Disulfides were selected as surface binding elements and Au as the surface in order to examine the consequences of surface binding both qualitatively and quantitatively. Benzoyl derivatives were chosen as polar elements, because their dipole moments can be varied regularly by varying the nature of the ring substituent. Palmitoyl moieties were selected as hydrophobic elements. In the following we establish the relationship among these molecules' structural characteristics, their mode of assembly on conducting and semiconducting surfaces, and the consequences of their assemblies on the substrates' surface properties. Toward this end we first examine these molecules' assemblies on gold, whose smooth and conducting surfaces enable us to apply ellipsometry, electrochemistry, and FTIR spectroscopy for characterization. The combination of these measurements provides a good estimate of the assemblies' thicknesses, the extent of surface coverage, and their orientation. We then compare the monolayers formed on gold with those formed on $CuInSe_2$ by comparing their contact angles and by deducing from these the coverage on the semiconductor. Finally we measure the contact potential differences imparted by each of the ligands on the two surfaces and show how these

differences can be directly correlated with the ligands' dipole moments, surface coverage, and orientation.

Synthesis. We synthesized the ligands by condensing *trans*-1,2-dithiane-4,5-diol with 1.1 equiv of either *p*-anisoyl chloride or *p*-cyano benzoyl chloride and 1.1 equiv of palmitoyl chloride. The resulting mixture of symmetric and asymmetric ligands was separated by chromatography and each of the products fully characterized by their spectral features. The formation of ester groups was confirmed by the C=O frequency of the products in the IR spectra. Ready distinction between the symmetric and asymmetric ligands was possible by ^1H NMR spectroscopy, and the identity of the compounds was further confirmed by mass spectrometry.

Characterization of Disulfide Assemblies on Gold. Determination of Monolayer Thickness, Surface Coverage, and Contact Angles. In order to establish the formation of disulfide assemblies on gold, we characterized the monolayers formed by each of the five compounds (Figure 1) with respect to ellipsometric thickness, wettability (advancing and receding contact angles (CAs) for water), and surface coverage, the latter being determined by metal underpotential deposition (UPD). The results of these measurements are summarized in Table 1.

The ellipsometric thickness values measured for the symmetric disulfides are close to those reported[39] for related compounds, namely, around 10 Å for the dipolar ligands **I** and **III** and 21 Å for the hydrophobic ligand **V**. The asymmetric ligands **II** and **IV** yielded thickness values around 14.5 Å, as expected for mixed monolayers consisting of extended benzoyl and palmitoyl residues. Some differences in coverage were observed for the different disulfides examined. Thus, the mixed monolayers derived from **II** and **IV** showed higher coverage than the homogeneous monolayers derived from the dipolar
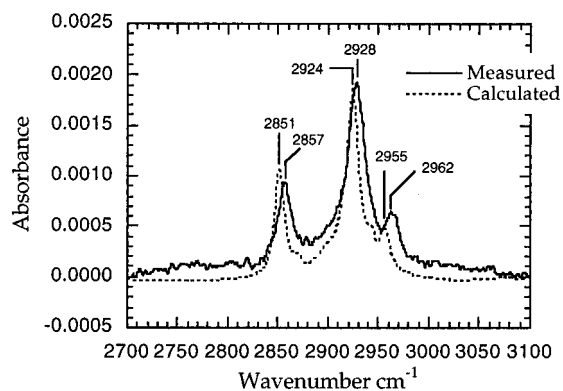
Figure 2. Grazing angle FTIR spectrum (3100−2700 cm⁻¹, hydrocarbon region) of an assembly of ligand **II** on a gold surface (solid line) along with a calculated spectrum of an isotropic assembly of this material (dashed line).

Figure 3. Grazing angle FTIR spectrum (3100−2700 cm⁻¹, hydrocarbon region) of an assembly of ligand **V** on a gold surface (solid line) along with a calculated spectrum of an isotropic assembly of this material (dashed line).

ligands **I** and **III**. Moreover, monolayers derived from disulfides possessing anisoyl residues **III** yielded higher coverage than those derived from disulfides possessing cyanobenzoyl residues **I**. The higher surface coverage observed in the mixed monolayer can be attributed to multiple, noncovalent interactions between the long alkyl chains, which are likely to align next to each other and form bundles. (This higher coverage may also be related to the higher hydrophobicity of these ligands, which prevents water, and hence the electroactive species, from reaching the electrode surface.) The higher coverage of the anisoyl derivative **III** than of the cyanobenzoyl derivative **I** might similarly reflect some favorable van der Waals interactions between the methoxy groups of the former or a higher hydrophobicity. The reasonably good coverage observed with the symmetric dianisoyl derivative **III** also allowed us to estimate the benzoyl groups' tilts relative to the surface normal. Inspection of the molecule's molecular model (giving an approximate height of 11 Å), and consideration of the observed thickness of 9.5 Å, yielded a tilt of 50° with respect to the surface normal.

Table 1 also presents the contact angles (H₂O) on assemblies on gold formed from each of the ligands applied. The assemblies made from the dipalmitoyl derivative **V** have the highest CAs because they contain two hydrophobic hydrocarbon chains.[82] The assemblies prepared from the asymmetric ligands **II** and **IV**, which contain one hydrocarbon chain, still show rather large CAs.[83,84] Thus, the presence of a single, long-chain fatty acid appears to be sufficient to screen the polar groups and significantly reduce wettability. The assemblies derived from the symmetric dipolar ligands show smaller CAs, with that of the dicyano derivative **I** being the smallest. This is consistent with the strong hydrophylic character of the exposed group in the latter ligands.

Determination of Ligand Orientation by FTIR. FTIR of the Hydrocarbon Region. Figures 2 and 3 show the grazing angle spectra (3100−2700 cm⁻¹, hydrocarbon region) of assemblies of ligands **II** and **V** on gold along with a calculated spectrum for an isotropic monolayer of these ligands. The calculated spectra were derived from the spectra of the compounds in KBr and Maxwell's equations.[79] Table 2 shows the assignments of peaks to particular modes of vibration. We concentrated on the CH₂ modes of vibration because the CH₃
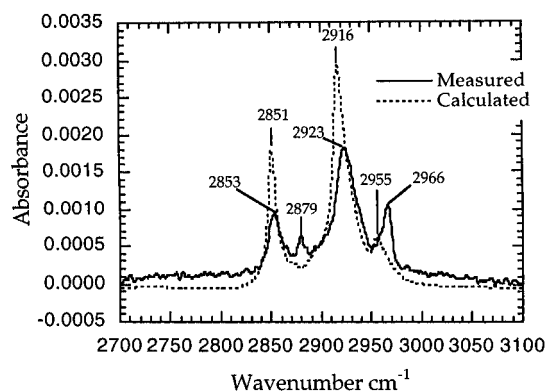
modes occur at the end of the chain where there should be fewer constraints on vibrational freedom. Particularly noteworthy is the fact that the CH₂ modes occur at higher wavenumbers in the assemblies than in the calculated spectra. (The calculated spectra were derived from solid phase spectra and show peak positions characteristic of the solid phase.) The shift to higher wavenumbers in assemblies relative to solids is ascribed to weaker intermolecular interactions.[39] Similar shifts in the peak positions of hydrocarbon infrared modes occur between the solid and the liquid phases because of an increase in freedom in the hydrocarbon modes.[85,86] The CH₂ modes in assemblies of ligands **II** and **IV** (not shown) occur at even higher wavenumbers than the CH₂ modes in assemblies of ligand **V** (as also observed in the solid state). This probably reflects greater conformational freedom of the hydrocarbon chain in the mixed hydrocarbon−aromatic ligands than in ligand **V**. In principle, one can calculate the orientation of the ligands in a monolayer using eq 1, where A is the measured absorbance, $A_{isotropic}$ is the

$$\frac{A}{3A_{isotropic}} = \cos^2 \phi \qquad (1)$$

theoretical absorbance for a randomly oriented monolayer, and ϕ is the angle between the dipole and the surface normal.[79] This method has been applied previously to calculate the orientation of the hydrocarbon chains of a monolayer of ligand **V**.[39] Assuming an all-trans conformation, we calculated the tilts given in Table 3 (but the spectra could also be explained if the hydrocarbon chains were rather isotropic). This configuration is suggested by the presence of the wagging and rocking modes between 1300 and 1200 cm⁻¹.[39,87] In the spectra of ligands **II** and **IV**, we do not see these modes, but they may be obscured by other peaks. The spectrum of the assembly of ligand **V** agrees very well with that reported earlier.[39] The difference in the magnitude of absorbances (a factor of 2) is well explained by the differences in the grazing angle used (here, 80°; in ref 39, 86°).

Midrange Spectrum (2300−1000 cm⁻¹). Figures 4 and 5 present the grazing angle FTIR spectra (2300−1000 cm⁻¹) of assemblies of ligands **II** and **III** along with the calculated spectra of an isotropic assembly. The Supporting Information contains the spectra of ligands **I** and **IV**. Many of the peaks in this region are due to aromatic ring stretches (see Table 2). As expected,

(82) Horr, T. J.; Ralston, J.; Smart, R. S. C. *Colloids Surf., A* **1995**, *97*, 183−196.

(83) Folkers, J. P.; Laibinis, P. E.; Whitesides, G. M. *Langmuir* **1991**, *7*, 3167−3173.

(84) Bain, C. D.; Troughton, E. B.; Tao, Y.-T.; Evall, J.; Whitesides, G. M.; Nuzzo, R. G. *J. Am. Chem. Soc.* **1989**, *111*, 321−335.

(85) MacPhail, R. A.; Strauss, H. L.; Snyder, R. G.; Elliger, C. A. *J. Phys. Chem.* **1984**, *88*, 334−341.

(86) Snyder, R. G.; Strauss, H. L.; Elliger, C. A. *J. Phys. Chem.* **1982**, *86*, 5145−5150.

(87) Snyder, R. G. *J. Mol. Spectrosc.* **1960**, *4*, 411−434.

Table 2. Assignments of Vibrational Modes and Transition Dipoles to Infrared Absorption Bands of the Disulfide Ligands[39,79,96]

| vibrational mode	absorption peak (cm^{-1})	transition dipole orientation
CH$_3$ asym stretch in the plane of the hydrocarbon backbone	2961−2966	⊥ C−CH$_3$ bond in the plane of the hydrocarbon backbone
CH$_3$ asym stretch out of the hydrocarbon backbone plane	2953−2957	⊥ hydrocarbon backbone plane
CH$_3$ sym stretch (Fermi resonance)	unresolved	‖ C−CH$_3$ bond
CH$_2$ asym stretch	2916−2928	⊥ plane of the hydrocarbon backbone
CH$_3$ sym stretch	2879−2883	‖ C−CH$_3$ bond
CH$_2$ sym stretch	2851- 2857	⊥ hydrocarbon chain in plane of backbone
C≡N stretch	2231−2237	‖ C≡N bond
C=O stretch	1715−1736	‖ C=O bond
aromatic ring mode	1607−1613	‖ ring 1,4 axis
aromatic ring mode	1581−1585	⊥ ring 1,4 axis
aromatic ring mode	1503−1514	‖ ring 1,4 axis
CH$_2$ scissors deformation	1466−1473	⊥ hydrocarbon chain
aromatic ring mode	1406 −1422	⊥ ring 1,4 axis
aromatic ring mode	1311−1328	⊥ ring 1,4 axis
C−O stretch	1268−1288	not well defined
C−O stretch (anisole)	1261−1268	‖ C−O bond

Table 3. Calculated Tilts[a,b] and Rotations[a] of the Alkyl Chains in Assemblies of Hydrophobic Ligands

	ligand		tilt angle	rotation angle
	R1	R2	(deg)	(deg)
II	*p*-cyanobenzoyl	palmitoyl	62	48
IV	anisoyl	palmitoyl	52	46
V	palmitoyl	palmitoyl	45	48

a To obtain the chain orientation, the chain axis was placed perpendicular to the surface with the plane of the backbone being in the *xz* plane. (The surface is the *xy* plane.) The alkyl chain was first tilted about the *y* axis by the tilt angle and then rotated about the chain axis by the rotation angle. *b* Calculations assume an all-trans conformation of the alkyl chain which may not be the case.
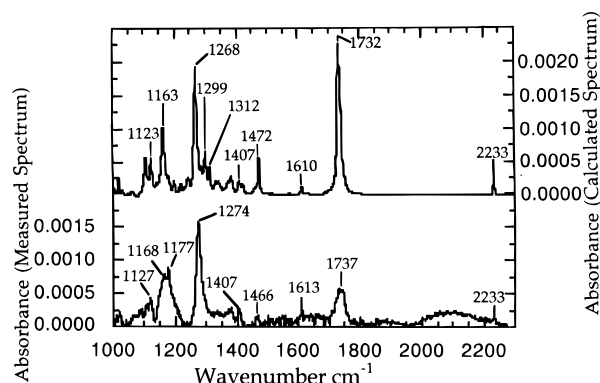
Figure 4. Grazing angle FTIR spectrum (2300−1000 cm^{-1}) of an assembly of ligand **II** on a gold surface (bottom) along with a calculated spectrum of an isotropic assembly of this material (top). Table 2 gives peak assignments in this region.

these peaks are higher in intensity for the assemblies which contain two benzene rings per ligand than for the mixed assemblies. The substitution of a second phenyl ring for the hydrocarbon chain of the mixed ligand increased the intensity of aromatic-associated peaks by factors between 1.5 and 3.0. We calculated the tilt of the phenyl ring with respect to the surface normal using eq 1. The tilt of the 1,4 axis can be calculated directly from several of the aromatic ring modes. Table 4 gives the results for the *p*-anisoyl-containing ligands (**III** and **IV**). The average tilts of the phenyl rings are 52° and 53° for ligands **III** and **IV**, respectively. The majority of the differences in the dipole moments of the ligands shown in Figure 1 derive from the aromatic ring(s) and their substituents, so that the tilt of the 1,4 axis is actually the quantity of interest. One must keep in mind that the tilt angles could easily vary by ±5°. We note that this FTIR-deduced tilt is very close to that derived from the monolayer's ellipsometric thickness, thereby giving confidence in the validity of the former approach. Calculations
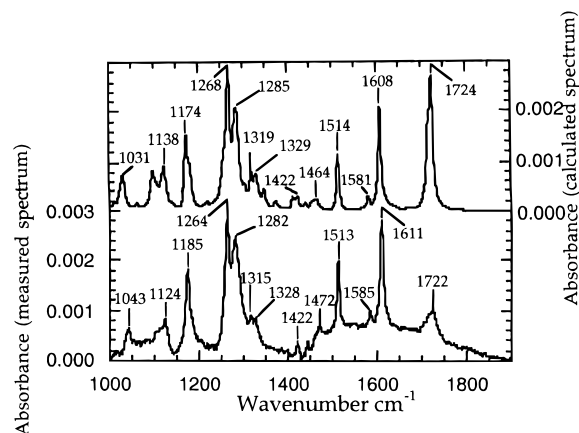
Figure 5. Grazing angle FTIR spectrum (1900−1000 cm^{-1}) of an assembly of ligand **III** on a gold surface (bottom) along with a calculated spectrum of an isotropic assembly of this material (top). Table 1 gives peak assignments in this region.

Table 4. Calculated Tilts of the Phenyl Rings' Main Axes in Assemblies of Polar Ligands

peak frequency (cm^{-1})	ligand			tilt of 1,4 axis from
	code	R1	R2	the surface normal
1611	**III**	anisoyl	anisoyl	51
1611	**IV**	anisoyl	palmitoyl	50
1513	**III**	anisoyl	anisoyl	53
1512	**IV**	anisoyl	palmitoyl	56

of the tilt for the *p*-cyanobenzoyl-containing ligands yielded inconsistencies as some measured peaks were greater than $3I_{calcd}$. Such inconsistencies were also observed by other groups[36] and may be due both to differences between absorption coefficients in the solid and in the assembly and to the noise level (for weak peaks).

Comparison between Disulfide Assemblies on Gold and on Semiconductors. Assemblies on CuInSe$_2$ do not lend themselves to the range of analyses possible with assemblies on gold, due to their surface roughness. However, meaningful contact angle measurements can nevertheless be performed and can be used to compare the nature of the assemblies on the two surfaces.

Inspection of the data in Table 1 shows that most of the contact angles are somewhat smaller on CuInSe$_2$ than on gold, with the exception of the bis(4-cyanobenzoyl) derivative I. Thus, the hydrophobicity of the ligands is less expressed on the CuInSe$_2$ surface than on Au. This could be due to differences in surface coverage or molecular orientation or a combination of both.

Several simple models have been proposed for the dependence of CAs on the scale of surface heterogeneities. In the case of heterogeneities much larger than the molecular dimensions, it was suggested[88] that the adhesion energies of the liquid should be averaged, yielding

$$\cos(\theta) = \sum_i f_i \cos(\theta_i) \qquad (2)$$

where θ is the CA on the heterogeneous surface, f_i is the fractional coverage of the ith molecule, and θ_i is the CA measured on a surface completely covered by this molecule.

In the case of heterogeneities on a molecular scale, it was proposed[89] that the polarizabilities of the molecules, instead of the cohesive energies, should be averaged, giving the expression

$$(1 + \cos(\theta))^2 = \sum_i f_i (1 \cos(\theta_i))^2 \qquad (3)$$

Note that both equations rely on crude approximations and overlook the microscopic features of the phenomena, like water−adsorbate interactions, which are very important in some instances.[60] Still, they are useful in attempting to make qualitative assertions more quantitative.

In order to obtain an estimate for the surface coverages in our systems, we assumed that (a) the binding to the substrate is weakly influenced by the substituents R1 and R2 (cf. Table 1) and (b) the CA is marginally dependent on the substrate at full coverage. The consequence of (a) is that the f_i values are a function of the substrate only while (b) means that the θ_i values are functions of the substituents only. Consider now a surface only partly covered by the adsorbate (**I−V**). If we compare the contact angles for the same molecule (**I−V**) on the two substrates, we get the relationship

$$\cos(\theta_{CISe}) = (f_{CISe}/f_{Au})\cos(\theta_{Au}) + K \qquad (4a)$$

or

$$(1 + \cos(\theta_{CISe}))^2 = (f_{CISe}/f_{Au})(1 + \cos(\theta_{Au}))^2 + K' \qquad (4b)$$

according to the chosen model (eq 2 or 3). K and K' are constants, independent of the specific substituents, but dependent on the coverage and on the CA of the bare substrate surfaces; θ_{Au} and θ_{CISe} are the measured CAs for the given molecule on Au and on CISe substrates, respectively.

We can now use the above relationships to obtain the coverage on CISe relative to that on Au substrates. To this end, we plot $\cos \theta_{CISe}$ versus $\cos \theta_{Au}$ according to eq 4a or eq 4b. Notwithstanding scatter in the data, this yielded similar graphs. The slopes of the linear regression curve fits fall between 0.4 and 0.5, for both advancing and receding angles, and thus suggest that coverage on CISe substrates is about half of that on Au.

Contact Potential Difference (CPD) Measurements. To establish the electronic consequences of ligand binding on both surfaces, we performed a series of CPD measurements. Figure 6 presents contact potential differences for gold films treated with the different disulfides as a function of the sum of the dipole moments of the ligands' substituents. A similar functional dependence is obtained when, instead of the dipole moments, the ligands' Hammett constants are used (not shown). Notwithstanding the introduction of two auxiliary functional groups, a good correlation is found between these parameters and the observed CPD changes. The difference between the
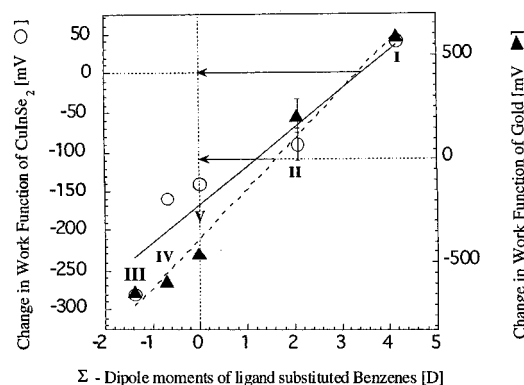
(88) Cassie, A. B. D. *Discuss. Faraday Soc.* **1948**, *3*, 11.
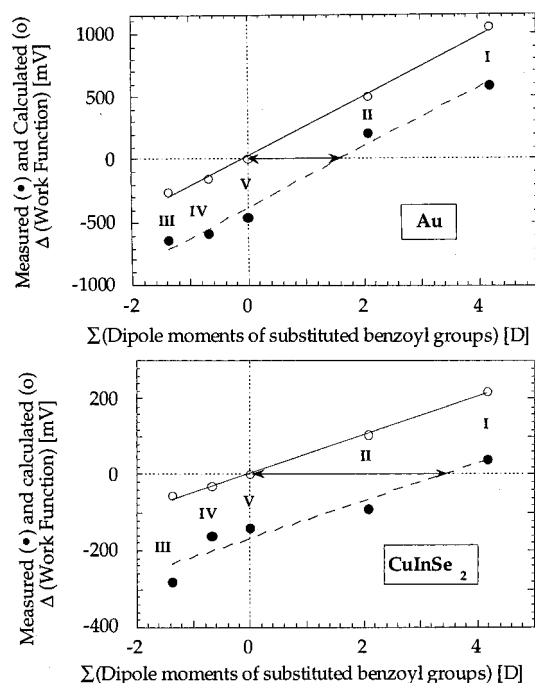(89) Israelachvili, J. N.; Michelle, L. G. *Langmuir* **1989**, *5*, 288−289.

Figure 6. Change in work function of gold and *p*-CuInSe$_2$ crystals as a function of the sum of the dipole moment of their substituted benzoyl groups.[64] The changes are with reference to bare gold and to CuInSe$_2$ treated with acetonitrile (to correct for a possible solvent effect, which might be present because of the low coverage). (Note the difference in the scales for CuInSe$_2$ and for Au.) The structures of the compounds are defined in Figure 1. The error bars represent the standard deviation from several measurements. For the sake of clarity, they are shown only for ligand **II**. The arrows show the residual dipole moments of the bound molecules, exclusive of the substituents.

surface potentials reaches the remarkably high value of 1.2 V upon treatment with the symmetric, dipolar ligands **I** and **III**. Adsorption of the asymmetric ligands **II** and **IV** results in surface potential differences of up to 800 mV. These changes in surface potentials are rationalized by the introduction of a layer of surface dipoles. Equation 5 describes the potential drop,

$$\Delta V = \frac{\mu \cos \varphi}{\epsilon \epsilon_o} \qquad (5)$$

ΔV, due to such dipole layers.

Here μ is the dipole moment per area, φ is the angle between the dipole and the surface normal, ϵ is the dielectric constant of the assembly−surface complex, and ϵ_o is the permittivity of free space.[90] Assuming that the surface contains a monolayer of ligands, the density of dipoles (benzene rings) is about 1 per 25 Å^2. The difference in dipole moment between *p*-cyanobenzoyl and *p*-anisoyl is 5.6 D.[91] Using this value in eq 5, the difference between the surface potential of gold films treated with ligands **I** and **III** could be as high as 1.6−2.2 V, depending on the value for the dielectric constant ϵ, which we estimate to be around 4−5.5.[92−94]

The observation of a lower than predicted value for the CPD changes (1.2 V instead of 1.6−2.2 V) between the two symmetric, dipolar ligands **I** and **III** could *a priori* derive from (i) incomplete surface coverage, (ii) tilts of the ligands' phenyl rings with respect to the surface normal (Table 4), or (iii) both. Considering the observed coverage of 75% and 85% for ligands **I** and **III**, respectively (Table 1), and the estimated tilts of ∼50° of the benzoyl rings relative to the surface normal (Table 4), the observed CPD changes agree well with the values calculated from eq 5, assuming $\epsilon = 4$ (Figure 7). Considering that the asymmetric ligands **II** and **IV** (i) show higher surface coverage, namely, 95% and 100%, respectively (Table 1), but (ii) possess

(90) Taylor, D. M.; Oliveira, O. N.; Morgan, H. *J. Colloid Interface Sci.* **1990**, *139*, 508−518.
(91) Weast, R. C. *CRC Handbook of Chemistry and Physics*, 57th ed.; CRC Press: Cleveland, OH, 1976; pp E-63−65.
(92) Demchak, R. J.; Fort, T. J. *J. Colloid Interface Sci.* **1974**, *46*, 191.
(93) Oliveira, O. N.; Taylor, D. M.; Lewis, T. J.; Salvagno, S.; Stirling, C. J. *J. Chem. Soc., Faraday Trans.* **1989**, *1009−1018*.
(94) *Landolt-Boernstein: Numerical Data and Functional Relationships in Science and Technology*, New Series ed.; Madelung, O., Ed.; Springer-Verlag: Berlin, Heidelberg, New York, 1991; Vol. Group IV, Vol. 6.

Control of Surface Potential and Wetting of Solids

J. Am. Chem. Soc., Vol. 119, No. 24, 1997 5727

Figure 7. Measured (●) and calculated (○) changes in the work function for Au (top) and CuInSe$_2$ (bottom) as a function of the sum of the dipole moments of the substituted benzoyl groups in the disulfide ligands. Measured values are those shown in Figure 6; calculated values are derived from eq 5 (see the text). A 50° tilt angle was used for all ligands for both surfaces, Au and CISe. This angle was derived from the ellipsometrically determined thickness (Table 1) and/or from FTIR data on Au (Table 4). Coverage on Au was derived from UPD measurements (Table 1) and coverage on CISe as 50% of that on Au (based on CA measurements). For both surfaces an area of 25 Å^2/molecule[19] and a dielectric constant of 4 (cf. the text) were used. The arrows show the displacement from the zero point for the unsubstituted ligand **V**, for which a dipole moment of zero is assumed. An additional factor of 0.4 was used for CISe to get the best fit to the slope of the experimental points (cf. the text).

only half the effective dipole moment of the symmetric ligands, the observed CPD changes, namely, 0.8 V, agree well with those derived from eq 5 (using the same tilt and ϵ values as for the symmetric ligands) (Figure 7).

Figure 6 also shows the change in the work function of *p*-CuInSe$_2$ after treatment with substituted disulfides (referenced to a crystal treated with solvent only). The changes in the semiconductor work function span 320 mV between extreme modifications and correlate well with the substituents' dipole moments (and Hammett parameters; data not shown). This result shows that control over the work function of single-crystal CuInSe$_2$ by changing the dipole moment of the adsorbed disulfides can be combined with grafting of an additional property onto the crystal. In principle, ligand adsorption on semiconductors can change electron affinity, band bending, or both. Using photosaturation measurements before and after ligand adsorption, we found that band bending was not changed upon surface treatment. Hence, the observed differences in work function are due to changes in electron affinity.

Comparing the plots for gold and for CuInSe$_2$ (Figure 6), it becomes apparent that the ligand-induced changes in work function are much larger on gold, 1.2 eV, than on CuInSe$_2$, 0.32 eV (similar results have recently been obtained for other semiconductor crystals such as GaAs or CdTe: Cohen, R.; et al. Unpublished results. Vilan, A. M.Sc. Thesis, The Weizmann Institute of Science, Rehovot, Israel, 1997). The difference between the effects on gold and on semiconductors might derive from (i) differences in the substrates' electrical properties

(i.e., screening) or (ii) differences in ligand adsorption. Electrostatic considerations exclude the possibility of screening because the molecules on the surface can be described as an infinite sheet of dipoles (i.e., an infinite flat plate capacitor), even if only uniform patches of localized dipoles exist on the substrate. Because there is no electric field outside of an infinite flat plate capacitor, there will be no rearrangement of charge in the metal to oppose the field. Thus, screening of the ligands' dipole field by the substrate's free carriers should not occur. Even if screening effects were operative, these effects should be higher on gold where there are more free carriers, and this would produce screening in a direction opposite to the effect seen here.

Therefore, the observed differences between the metal and semiconductor likely derive from differences in ligand adsorption: the extent of coverage and the molecules' orientation and mode of binding. Contact angle measurements (Table 1) suggest that the coverage on CuInSe$_2$ is about half of the coverage on gold, thereby reducing the ligands' effects (although this accounts for only half of the observed differences between CuInSe$_2$ and gold). The lower surface coverage could result from the larger spacing of the surface elements that bind to the disulfide groups. Further reduction in CPD changes on CuInSe$_2$ could result from higher tilt angles due to the lower coverage. Additionally, the mode of ligand binding must also be inherently different, as the disulfides bind to gold on the one hand but to partially ionic indium on the other hand. Finally the structures and morphologies of the two surfaces will be quite different, as expressed, *inter alia*, in the observed differences of surface roughness for CISe and Au (from SEM measurements; cf. also ref 19).

In plots analogous to those of Figure 6, but for the binding of benzoic acid derivatives to CdTe, CdSe, CuInSe$_2$,[19,20] and GaAs,[97] the ligand lacking substituents on the para position of the benzoyl group does not necessarily give a zero change in electron affinity. For the disulfides discussed here we can take ligand **V** as the reference molecule with zero dipole moment of its substituents. Here again, ligand **V** does not give a zero change in electron affinity, also when its interpolated value is considered. For Au the difference is nearly 400 mV, and for CuInSe$_2$ it is nearly 200 mV. These changes in electron affinity are likely due to combinations of the following factors: (i) variability in the value of the reference sample and uncertainty in its choice (e.g., etched CuInSe$_2$ vs solvent only treated CuInSe$_2$), which would shift the plot of the change in CPD vs dipole moment along the ΔCPD axis (*y* axis), (ii) the presence of additional, molecular dipole moments, which will give a shift along the dipole axis (*x* axis). These additional dipole moments can be due to (i) the fixed parts of the molecules, namely, the molecules' backbone exclusive of the benzoyl and/or palmitoyl residues, and/or (ii) to the ligand−substrate bonds.

The shifts due to a dipole of the molecules' backbone should be similar for all molecules on both substrates, after taking into account differences in tilt angles and coverage (cf. eq 5). The shifts due to ligand−substrate bonds, on the other hand, should depend on the substrate. Assuming that the ligands bind directly to Au and In, we can deduce values of 2.5 D for the In−S bond and close to 0 D for the Au−S bond, using electronegativity differences.[74] From the plot we find zero change in work function at +1.6 D for Au and +3.5 D for CISe. This suggests that 1.5 D can be attributed to the invariant molecular backbone of the molecules.[95]

We can now use the data that we have gathered, i.e., (i) the average tilt of the molecules as suggested by a combination of ellipsometric thickness and FT-IR (50°), (ii) the extent of

coverage as determined electrochemically and from CAs, and (iii) the sum of the dipole moments of the substituents of the ligands (cf. Figure 6), and calculate the ΔCPD from eq 5, using $\epsilon = 4$ (as discussed above). By ignoring any residual dipole moment in the molecule, we put ligand **V** at ΔCPD = 0. The calculated and measured values for Au and for CISe are shown in Figure 7 (top and bottom, respectively). For CISe the best fit (in terms of slope) was obtained by scaling the calculated values by a factor of 0.2, although the estimated coverage on CISe relative to gold (approximately 50% of that on Au) would be in agreement with a factor of 0.5. This disagreement is most likely to derive from differences in ligand adsorption, larger tilts of the molecules on CISe than on Au, different modes of ligand binding, and different morphologies, as more explicitly elaborated above.

It can thus be concluded that the work function changes imparted by surface binding molecules can be predicted from their substituents' dipole moments, provided the molecules' binding groups and modes of interaction with the surface are known. Moreover, this predictive capability validates our initial hypothesis that molecular modifications of solid surfaces can be considered to be composites of a set of separate variables that can be modified separately and independently.

Conclusions

Adsorption of asymmetric, cyclic disulfides on surfaces provides stoichiometrically defined, homogeneously mixed assemblies, whose properties are controlled by the disulfides' substituents. The dipole moment of one substituent controls the substrates' surface potentials, while the hydrophobicity of the second substituent reduces the surfaces' wettability. Thus, control of more than one surface property was achieved with a mixed assembly.

---

(95) As one of the reviewers suggested, we can also consider the shifts along the *y* axis. The overall CPD changes for zero dipole moment are 380 mV for Au and 170 mV for CISe, using the linear curve fits shown in Figure 6. Neglecting variabilities and uncertainties in the selection of the reference samples, the shift for Au is attributed to the molecules' residual dipole moments exclusive of the benzoyl and palmitoyl substituents and the shift on CISe to both the molecules' residual dipole moments exclusive of the benzoyl and palmitoyl substituents and the dipole moment of the In−S bond. The latter contribution will be scaled according to the tilt of the bond relative to the surface normal; see eq 5. The numerically larger effect on Au relative to CISe can be attributed to the twice as large coverage on Au relative to CISe and to the difference in structure and morphology (including roughness) between the surfaces.

(96) Daimay, L.-V.; Colthup, N. B.; Fateley, W. G.; Graselli, J. G. *The Handbook of Infrared and Raman Characteristic Frequencies of Organic Molecules*; Academic Press: Boston, 1991.

(97) Bastide, S.; Butruille, R.; Cahen, D.; Dutta, A.; Libman, J.; Shanzer, A.; Sun, L.; Vilem, A. *J. Phys. Chem. B* **1997**, *101*, 2678−2684.

Adsorption of asymmetric ligands on gold caused surface potential changes over a range of 0.8 V, and adsorption of the same ligands on $CuInSe_2$ caused changes of 0.1 V. The symmetric dipolar ligands changed the surface potentials of gold by 1.2 V between extreme modifications and the surface potential of $CuInSe_2$ by 0.3 V. The magnitude of these effects can be described quantitatively by a simple electrostatic model which correlates the observed CPD changes with the dipole moments of the ligands' substituents, their tilts relative to the surface normal, and the ligands' surface coverage. The induced CPD changes per benzoyl substituent are larger for the asymmetric than for the symmetric dipolar ligands, due to the formers' superior surface coverage. By the same token, the larger effects on gold relative to $CuInSe_2$ are similarly attributed to higher coverage.

The results presented above validate our working hypothesis that it is indeed possible to control two surface properties by chemisorption of tailor-made molecules that possess (i) functional groups for surface binding and (ii) two distinct auxiliary groups for surface modifications. Such molecules form homogeneously mixed monolayers that do not segregate and thereby impart simultaneously two desired properties, such as work function changes and diminished wettability. Current efforts are aimed at applying this methodology for the generation of organized assemblies that possess a variety of desired functionalities such as light-absorbing and light-emitting elements, catalytically active and optically active elements, or hydrophobic and anisotropic groups that act in concert.

Supporting Information Available: Additional experimental details on FTIR measurements and additional FTIR results (grazing angle FTIR spectra of assemblies of **I** and **IV** (2 pages). See any current masthead page for ordering and Internet access instructions.

JA964434Z